J Nanopart Res (2018) 20: 263
https://doi.org/10.1007/s11051-018-4333-0

RESEARCH PAPER

The time-dependent cellular response mechanism upon exposure to zinc oxide nanoparticles

Zi-jin Zhang · Zhi-jie Tang · Zhen-yu Zhu · Zhao-ming Cao · Hong-juan Chen · Wei-juan Zheng · Xin Hu · Hong-zhen Lian · Li Mao

Received: 5 April 2018 / Accepted: 17 August 2018 / Published online: 26 September 2018

Abstract Zinc oxide nanoparticle is one of the nanomaterials people engaged most in their life and its health effect has been taken into concern. In this work, A549 cell line was used as cell model, and the cytotoxicity of zinc oxide nanoparticles was revealed to be concentration-dependent. Through the measurement of cellular proteome, much more differentially expressed proteins were observed after the cells being treated for 9 h than 24 h. Also, most of these proteins expressed in the pattern which showed a significant decrease after exposure to zinc oxide nanoparticles and then an increase at 24 h. Intracellular reactive oxygen species and glutathione determination indicated that high level of oxidative stress was presented in cell after treatment with zinc oxide nanoparticles for 9 h. It can be observed from western blot analysis that the expression of NF-κB p65, PNPase, and HSP90 rose significantly after 9 h of exposure. Thus, a deduction was reached that toxicity of nanoparticles consists both of particle toxicity and ion toxicity, and a long-time treatment may conceal the toxicity induced by particles. The conclusion we made highlighted the importance of exposure time in the study of nanoparticle toxicity and would provide a new perspective for studying toxicity mechanism of nanoparticles.

Keywords Zinc oxide nanoparticles · iTRAQ · Proteomics · Toxicity · Time-dependent response · Health effects

Electronic supplementary material The online version of this article (https://doi.org/10.1007/s11051-018-4333-0) contains supplementary material, which is available to authorized users.

Z.-j. Zhang · Z.-j. Tang · Z.-m. Cao · X. Hu · H.-z. Lian (✉)
State Key Laboratory of Analytical Chemistry for Life Science, Collaborative Innovation Center of Chemistry for Life Sciences, School of Chemistry and Chemical Engineering and Center of Materials Analysis, Nanjing University, Nanjing 210023, China
e-mail: hzlian@nju.edu.cn

Z.-y. Zhu · H.-j. Chen · W.-j. Zheng
State Key Laboratory of Pharmaceutical Biotechnology, School of Life Sciences, Nanjing University, Nanjing 210023, China

L. Mao (✉)
Ministry of Education (MOE) Key Laboratory of Modern Toxicology, School of Public Health, Nanjing Medical University, Nanjing 211166, China
e-mail: maoli@njmu.edu.cn

Introduction

Recent innovations in mass production of nanoparticles have led to rapid commercialization of these kinds of materials with characteristic length less than 100 nm (Meyer, et al. 2009). As a result, nanoparticles are now widely used in industrial and commercial fields. Due to the rising application of nanoparticles, their health and environment effect has been taken into concern. A large number of studies have been taken to evaluate the toxicity of nanomaterials both in vivo and in vitro. It was reported that ultrafine carbon black induced lung injury in mice (Chang, et al. 2007). Titanium oxide nanoparticles were found to cause cell death in BEAS-2B cells (Park, et al. 2008) and reduced cell viability

was showed in silica nanoparticle-treated A549 cells (Lin, et al. 2006).

Zinc oxide nanoparticles are one kind of most concerned nanomaterials among them since its application in commodities such as paints, cosmetics, batteries, sunscreens, and electronic devices (The Project on Emerging Nanotechnologies Consumer Products Inventory, http://www.nanotechproject.org/inventories/consumer/). However, a great number of studies have shown its toxicity in vitro (Zhong, et al. 2017). For instance, LDH leakage and a great reduction in cell viability were caused by ZnO nanoparticles while using Neuro-2A mouse neuroblastoma cell line as cell model (Jeng and Swanson, 2006); ZnO nanoparticle-induced cytotoxicity was also observed in THP1 human monocytic cell line (Prach, et al. 2013); Primary human nasal mucosa cells showed DNA damage and inflammation after treatment with ZnO nanoparticles (Hackenberg, et al. 2011).

Although great effort has been put on toxic effect of zinc oxide nanoparticles, the toxicity mechanism still remains unclear. Two explanations on zinc oxide nanoparticle toxicity are now proposed by researchers. Many researchers consider zinc ions as the main cause of zinc oxide nanoparticle toxicity. For example, Song et al. found that supernatants of zinc oxide nanoparticles induce 50% cell death so that the dissolved zinc ions played a main role in toxic effect of zinc oxide nanoparticles in Ana-1 mouse macrophage cell line. In addition, they thought that reactive oxygen species (ROS) generation is not enough to cause cytotoxicity though it had a good correlation with cell viability reduction (Song, et al. 2010). Same mechanism was concluded by Deng et al. since they found that zinc oxide nanoparticles showed similar toxic effect on C17.2 mouse neural stem cell line and engulfed particles could hardly be visualized in TEM images (Deng, et al. 2009). A great number of studies also support the leading role of zinc ions in zinc oxide nanoparticle toxicity (Xia, et al. 2008; Triboulet, et al. 2014; Cho, et al. 2012). However, some other researchers focused on the ROS-induced damage in cells, which is mainly caused by particles due to its high specific surface area (Nel, et al. 2006). Sharma et al. discovered that the toxicity induced by zinc oxide nanoparticles in HepG2 human liver cell line was concentration- and time-dependent. Furthermore, a significant increase in ROS and DNA damage was detected, thus suggesting the role of particles in the zinc oxide nanoparticle toxicity mechanism (Sharma, et al. 2011). Elevating oxidative stress, cell membrane damage, and intracellular $[Ca^{2+}]_{in}$ in a concentration- and time-dependent fashion in BEAS-2B human bronchial epithelial cell line after treatment with zinc oxide nanoparticles was observed by Huang et al., and addition of antioxidant N-acetyl-L-cysteine (NAC) can completely abolish the cytotoxicity. Moreover, the increase of $[Ca^{2+}]_{in}$ had a good correlation with cytotoxicity, and was partially reversed by NAC treatment, which built the connection with the oxidative stress (Huang, et al. 2010). Lin et al. found that zinc oxide nanoparticle treatment caused significant reduction in A549 human lung adenocarcinoma cell viability, and particle mass-based dosimetry and particle-specific surface area-based dosimetry yielded two distinct patterns of cytotoxicity in both 70 and 420 nm zinc oxide nanoparticles. They also discovered that the elevation of ROS resulted in intracellular oxidative stress, lipid peroxidation, cell membrane leakage, and oxidative DNA damage, while NAC could protect cells from zinc oxide nanoparticle-induced toxicity. Furthermore, they found that the dissolution of zinc oxide nanoparticles was not enough to cause significant cytotoxicity, and they concluded that particles are major contributors to zinc oxide nanoparticle toxicity (Lin, et al. 2009). There is no doubt that both nanoparticles and ions can cause direct toxicity to cells, but under what situation should one of them show more importance in toxicity need to be studied deeply.

On the other hand, few researchers have used proteomic method, a powerful tool for us to have an overall view of the effect induced by zinc oxide nanoparticles to study the toxicity mechanism of zinc oxide nanoparticles. Triboulet et al. used two-dimensional gel electrophoresis to investigate the proteome changes in RAW264 macrophage. They found a rather weak response in oxidative stress response pathway but strong responses both in central metabolism and in proteasome protein degradation pathway, while carbohydrate catabolism and proteasome are critical in response to zinc ions. By contrast, glutathione level and phagocytosis did not show significant changes at moderately toxic zinc concentration. It is concluded that zinc ions bound proteins and induced impairment of central metabolism and thus mainly contributed to the zinc oxide nanoparticle toxicity, and proteasome plays an important role in zinc resistance (Triboulet, et al. 2014).

Considering the various results coming out before, our work chose A549 cells as subject, profiled the proteome after different period of treatment with zinc

oxide nanoparticles, and analyzed the intracellular ROS level in order to verify the result. We aimed to study the toxicity mechanism of zinc oxide nanoparticles and tried to explain the divergence in previous works.

Materials and methods

Zinc oxide nanoparticles

Zinc oxide nanoparticles were purchased from Sigma-Aldrich (catalog 544906). Nanoparticles were dispersed in water as a suspension by sonication for 30 min. The concentration was determined after digestion with concentrated hydrochloric acid using an inductively coupled plasma atomic emission spectroscopy (ICP-AES, PerkinElmer SCIEX, Optima 5300). Elemental composition of zinc oxide nanoparticle was determined by an energy dispersive X-ray spectroscopy (EDX, HORIBA, EX250). The morphology of nanoparticles was observed by a scanning electron microscopy (SEM, Hitachi, S-3400N II) and a transmission electron microscopy (TEM, JEOL, JEM-200CX). The hydrodynamic diameter (Dh) of zinc oxide nanoparticles was determined by dynamic light scattering (DLS) experiment using a particle size analyzer (BIC, NanoBrook 90 Plus PALS).

Cell culture and treatment with zinc oxide nanoparticles

Human lung adenocarcinoma cell line A549 was purchased from Cobioer Biotech (Nanjing, China) and were maintained in the complete cell culture medium F12-K supplemented with 10% fetal bovine serum, 100 units/L penicillin, and 0.10 mg/mL streptomycin at 37 °C in a humidified 5% carbon dioxide (CO_2) atmosphere. All cell samples were prepared using at least three replicates for an experiment. A stock solution of up to 1.22 g Zn/L was prepared and dispersed for 30 min by a sonicator to prevent aggregation, and diluted to the specified concentrations (1, 2.5, 5, 10, 25, 50 mg Zn/L) for treatment of cells.

Cell viability assays

Cellular viability was determined using the CCK-8 assay and Annexin V-FITC/PI staining (Beyotime). Cells were seeded with equal density in each well of 96-well plates (5×10^3 cells per well), 100 μL of cell culture medium per well, and incubated for 24 h at 37 °C. Then, cells were treated in 96-well plates with 1 mg Zn/L, 2.5 mg Zn/L, 5 mg Zn/L, 10 mg Zn/L, 25 mg Zn/L, or 50 mg Zn/L of zinc oxide nanoparticles for 24 h at 37 °C. The medium was renewed with fresh culture medium before assay and 10 μL CCK-8 solution was added to each well, and the plate was incubated for 30 min at 37 °C. Subsequently, the absorbance was measured at 450 nm using a Bio-Rad 680 enzyme micro-plate reader. Cell viability was calculated by comparing absorbance value of cells treated with nanoparticles and untreated cells, and the cell viability of untreated cells was as 100%. Another group of nanoparticle-treated cells were collected and resuspended using PBS. 10^5 cells were taken and centrifuged. The supernatants were discarded and 195 μL Annexin V buffer, 5 μL Annexin-FITC, and 10 μL PI staining solution were added to each sample and mixed. After being incubated for 20 min in a dark place at room temperature, the samples were measured on a flow cytometer (Becton Dickinson, FACSCalibur).

Preparation of protein samples

Cell lysis was applied using a cell lysis kit (Beyotime, Haimen, China). Briefly, cells were washed with ice-cold PBS after removing the cell culture medium. Then, 1 mL cell lysis buffer (20 mM Tris (pH 7.5), 150 mM NaCl, 1% Trition X-100, Inhibitor (sodium pyrophosphate, β-glycerophosphate, EDTA, Na_3VO_4, and leupeptin)) was added and cells were harvested after 1 min. Lysates were sonicated for 1 min at a 10% amplitude at interval settings of 2 s on and 3 s off with a sonicator. The heat generated by sonication was below 1000 J. The supernatants were clarified and recovered after centrifugation at 15000×*g* for 30 min at 4 °C. Protein samples were flash-frozen and stored at − 80 °C. The concentration of the protein extracts was determined using the BCA method.

iTRAQ (isobaric tags for relative and absolute quantification)

An aliquot (200 μg) of acetone-precipitated protein sample was reduced with 4 μL of reducing reagent (AB Sciex, Redwood City, CA, USA) at 60 °C for 1 h. 2 μL of cysteine-blocking reagent (AB Sciex, Redwood City, CA, USA) was then added. After reaction for 10 min, samples were centrifuged at 12000 rpm for 20 min and bottom solution was disposed. Protein for each sample

was digested with trypsin overnight at 37 °C in a 1:50 trypsin-to-protein mass ratio. iTRAQ Reagent was then added and samples were dried by vacuum centrifugation after incubation for 2 h. The proteins were labeled with iTRAQ tags as follows: control group, Tag113; 9-h group, Tag114; 24-h group, Tag115.

Labeled peptides were resuspended with loading buffer (20 mM ammonium formate, pH 10) and loaded onto a Durashell C18 column (4.6 mm × 150 mm, particle size 5 μm) at 0.8 ml/min. Peptides were eluted from the analytical column after a 65-min reverse phase solvent gradient from 5% B (A: 20 mM ammonium formate, B: 20 mM ammonium formate, 80% acetonitrile) to 90% B. Peptides were then resuspended and loaded onto a TripleTOF TM 5600 mass spectrometer (AB Sciex, Redwood City, CA, USA). TOF MS was performed under the following condition: m/z: 350–1250, accumulation time: 0.25 s.

Proteomic data analysis and bioinformatics

Raw data of iTRAQ-labeled proteins were processed for database searching using Mascot (Matrix Science, London, UK). The search parameters were set as follows: cysteine alkylation with IAM; trypsin digestion; maximum of two missed cleavage sites; 0.02 Da fragment mass tolerance. A decoy database search strategy was used to determine the false discovery rate (FDR) for peptide and protein identification. Peptide identifications were accepted if their FDR value was < 1.0%, while protein identifications contained at least 1 identified peptide. Protein quantification required a p value < 0.05, only fold-change ratios > 1.500 or < 0.667 were considered statistically significant. GO annotations for the identified proteins were assigned according to those reported in the UniProt database (http://www.uniprot.org). The differentially expressed proteins that we identified were categorized according to the DAVID Classification System (https://david.ncifcrf.gov/). Pathway analyses of identified proteins were performed using the Kyoto Encyclopedia of Genes and Genomes (KEGG) database (http://www.genome.jp/kegg/). GO terms and KEGG pathways with corrected p value < 0.05 were considered significant.

Western blot

Thirty-five micrograms of proteins in whole cell extracts were fractionated on 12% acrylamide gels by sodium dodecyl sulfate-polyacrylamide gel electrophoresis (SDS-PAGE) according to Laemmli's method (Laemmli, 1970). Proteins were then electrotransferred on to PVDF membranes using a Mini P-4 electrotransfer apparatus (Cavoy, Beijing, China). PVDF membranes were activated by soaking in methanol for 1 min prior to blotting. The membranes were then equilibrated for 30 min in blotting buffer [48 mM Tris-base, 39 mM glycine, 20% (v/v) methanol, and 0.0375 (w/v) SDS]. A "blotting sandwich" was made according to the manufacturer's instructions. Blotting was carried out for 1 h on ice at a constant voltage of 300 mA. After transfer, the membrane was blocked in western blocking buffer for 1–2 h at room temperature. After three washing steps with PBST (PBS with Tween-20) for 10 min, the membrane was incubated with primary antibody overnight at 4 °C. The primary antibodies were diluted in primary antibody dilution buffer as ratio of 1:500 according to manufacturer's specifications. Then, the membrane was washed three times with PBST for 10 min and incubated for 1 h at room temperature in the presence of the appropriate horseradish peroxidase-conjugated secondary antibody. After several washes, the membrane was incubated with Tanon High-sig ECL Western Blotting Substrate (Tanon, Shanghai, China) and immune complexes were detected using the Tanon 6200 chemiluminescence workstation (Tanon, Shanghai, China).

Intracellular ROS measurement

The intracellular ROS was determined using a well-characterized probe, 2′,7′-dichlorofluorescin diacetate (DCFH-DA). DCFH-DA passively enters the cell, and is hydrolyzed by esterases to DCFH. This nonfluorescent molecule is then oxidized to fluorescent compound dichlorofluorescein (DCF) by cellular oxidants. A DCFH-DA stock solution of 10 mM was diluted 1000-fold in the cell culture medium without serum or other additives to yield a 10 μM working solution. Cells were washed three times with PBS and then incubated with 1 mL DCFH-DA working solution for 30 min in the 37 °C incubator. Then, the cells were washed three times with cell culture medium without serum to eliminate DCFH-DA that did not enter the cells. Cells were harvested and the fluorescence was determined at 488 nm excitation and 525 nm emission using a fluorospectrophotometer (Shimadzu, RF-5301PC).

Total glutathione and oxidized glutathione measurement

Intracellular total glutathione and oxidized glutathione (GSSG) was detected using a total glutathione and oxidized glutathione assay kit (Beyotime, Haimen, China). Glutathione (GSH) can reduce 5,5′-dithiobis-(2-nitrobenzoic acid) (DTNB) to yellow 5-thio-2-nitrobenzoic acid (TNB) and be oxidized to GSSG, and addition of glutathione reductase can reduce GSSG to GSH, so that the reaction rate was limited to the amount of total glutathione (GSH + GSSG), which thus can be detected according to the absorbance. In addition, presence of tris(2-hydroxyethyl) amine and 2-vinylpyridine can abolish GSH and, as a result, the amount of GSSG can be observed. Briefly, cells were washed with PBS and then collected. Supernatants were discarded after centrifugation and 30 μL protein eliminating solution was added. The samples were then flash-frozen to − 80 °C and melt under 37 °C water bath, twice, and put in the 4 °C environment for 5 min. The samples were further centrifuged at 10000×*g* for 10 min at 4 °C, and the supernatants were collected. Subsequently, the absorbance was measured at 412 nm. Intracellular total glutathione and oxidized glutathione was calculated by comparing absorbance value of cells treated with nanoparticles and untreated cells.

Statistical analyses

All measurements were repeated at least three times and data were expressed as mean ± SEM. Statistical significance for comparison of two groups was assessed using one-way ANOVA with the Tukey–Kramer multiple comparison post hoc test. Differences that were considered to be statistically significant are indicated as follows: *, $p < 0.05$ vs. untreated controls.

Results

Characterization of zinc oxide nanoparticles

SEM and TEM micrographs showed that zinc oxide nanoparticles were spherical and had a diameter about 30 nm (Fig. 1). The EDX analysis (Fig. S1 and Table S1, see Supplementary Material) showed that the major elemental composition (> 98%) of zinc oxide nanoparticles was zinc and oxygen with minor amount of aluminum. The DLS analysis (Table S2 and S3, see Supplementary Material) showed that zinc oxide nanoparticles are relatively stable in culture medium (F12K + 10% FBS).

In order to verify that zinc oxide nanoparticles had not dissolved before they contacted the cells, the supernatants of stock solution (1.22 g Zn/L) were measured after being stored for 7 days and the concentration of zinc ions was only 7.58 mg/L.

Cell viability

Cytotoxicity induced by zinc oxide nanoparticles was estimated as shown in Figs. 2 and 3. Treatment with zinc oxide nanoparticles at the concentration below 5 mg Zn/L for 24 h failed to induce significant reduction of A549 cell viability and less than 5% cell death was observed. However, 10 mg Zn/L zinc oxide nanoparticles significantly decreased cell viability. And as the concentration of nanoparticles increased, the cell viability dropped continuously. The cell viability was about 60% at the dosage of 25 mg Zn/L and nearly half of cell death could be observed at the dosage of 50 mg Zn/L (Fig. 2). According to the result of flow cytometry, 96.5% cells were viable after being treated with 5 mg Zn/L for 24 h while only 76% cells were viable when the concentration rose to 25 mg Zn/L (Fig. 3). Accordingly, we chose 5 mg Zn/L zinc oxide nanoparticles, which is considered to be sub-cytotoxic and can reduce the cell impairment to a minimum in order to analyze the protein regulation for further research of toxic mechanism in the following experiments.

Proteome expression patterns in response to zinc oxide nanoparticles

iTRAQ assay was conducted in order to further evaluate the effect of zinc oxide nanoparticles on proteome of A549 cells. Five milligrams zinc per liter of zinc oxide nanoparticles was used to treat cells for 9 h and 24 h according to our previous work which revealed that the response to sub-cytotoxic zinc ions of A549 cells reached its maximum at about 8–10 h. On the other hand, this can help us compare the proteome differences induced by zinc oxide nanoparticles and zinc ions and further study the toxicity mechanism of zinc oxide nanoparticles (Zhao, et al. 2014; Zhao, et al. 2015).

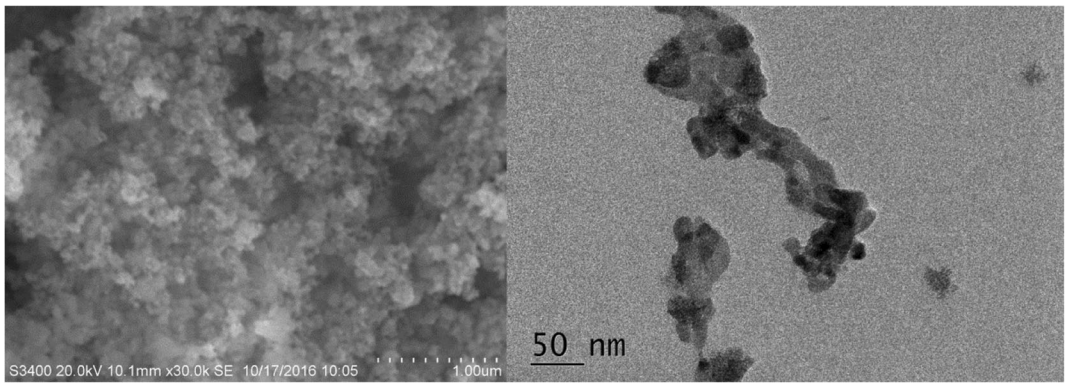

Fig. 1 SEM (left) and TEM (right) images of zinc oxide nanoparticles

Four thousand thirty-two proteins were identified through the assay, in which 120 were differentially expressed proteins ($p < 0.05$, fold-change > 1.500 or < 0.667). Among them, 99 were presented in the 9-h group, in which 12 (12.1%) were up-regulated while rest 87 (87.9%) were down-regulated; 41 were presented in the 24-h group and 9 (22.0%) of them were up-regulated while rest 32 (78.0%) were down-regulated. Twenty proteins were identified differentially expressed both after 9 h and 24 h, in which 3 were up-regulated proteins that showed higher expression after 24 h of treatment than 9 h, while 2 proteins (11.8%) among the rest 17 down-regulated proteins showed lower expression after 24 h of treatment compared to 9 h, and the rest 15 proteins (88.2%) showed an up-regulation that took place at 24 h compared to 9 h, though still down-regulated compared to the control group. Detailed differentially expressed proteins are shown in the Supplementary Material, Table S4 and S5, and a clear view of the change of protein expression is showed in Fig. S2.

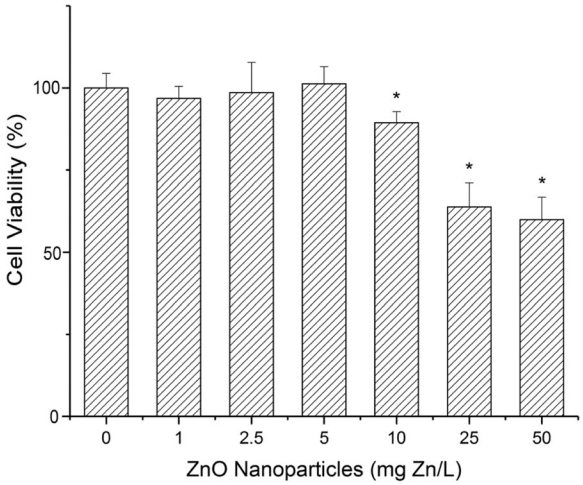

Fig. 2 Cell viability analysis of A549 cells after treatment with zinc oxide nanoparticles

Functional classification of differentially expressed proteins

Multiple function analyses of identified differentially expressed proteins were performed. The differentially expressed proteins that we identified were categorized according to the DAVID Classification System (https://david.ncifcrf.gov/) and a great number of biological processes were changed significantly after treatment with zinc oxide nanoparticles, including cell-cell adhesion (GO:0098609), glycolytic process (GO:0006096), gluconeogenesis (GO:0006094), rRNA processing (GO:0006364), response to unfolded protein (GO:0006986), cell redox homeostasis (GO:0045454), and many processes directly engaged in protein synthesis, for example, translation (GO:0006412), protein folding (GO:0006457), etc. Fig. S3 shows some main biological processes involved in response to zinc oxide nanoparticles. In addition, molecular functions of differentially expressed proteins were also studied, including protein binding (GO:0005515), RNA binding (GO:0003723), oxidoreductase activity, acting on the CH-OH group of donors, NAD or NADP as acceptor (GO:0016616), ion channel binding (GO:0044325), kinase binding (GO:0019900), etc. Detailed information is shown in Supplementary Material, Table S6-S9. Besides, KEGG System (http://www.genome.jp/kegg/) was used to investigate the pathway these differentially expressed proteins participated in, which includes glycolysis/gluconeogenesis (hsa00010), pyruvate metabolism (hsa00620), RNA degradation (hsa03018),

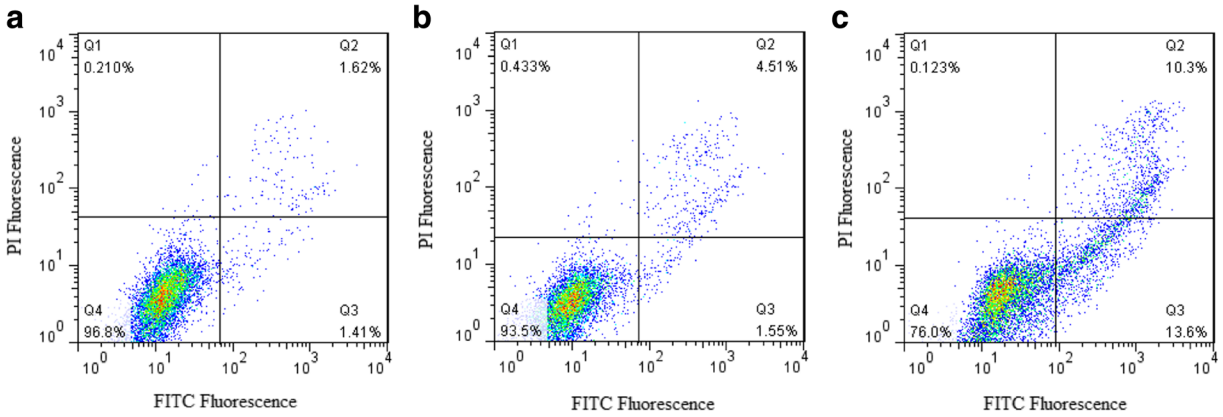

Fig. 3 Two-color flow cytometry analysis of A549 cells after treatment with 0 (**a**), 5 (**b**), and 25 mg/L (**c**) zinc oxide nanoparticles

etc. Detailed lists of pathways can be found in the Supplementary Material (Table S10 and S11).

Expression of HSP90, NF-κB p65, and PNPase

The expression of heat shock protein 90, nuclear factor-kappa B, and purine nucleoside phosphorylase were observed after A549 cells were treated with zinc oxide nanoparticles for 9 h and 24 h. The relative abundance of proteins treated with nanoparticles compared to the internal reference protein beta-actin was analyzed and normalized. These differential expression patterns are shown in Fig. 4. Exposure to zinc oxide nanoparticles produced a peak value of Hsp90 after 9 h, which was about a twofold increase, and then decreased to the level of control group after 24 h of treatment. Statistical analysis revealed significant differences in abundance of Hsp90 after treatment for 9 h. The expression of NF-κB p65 and PNPase showed a similar pattern. It increased about 40% after treatment for 9 h with significant differences, and then dropped significantly to about only 60% of the control group level. Two proteins both showed a response to zinc oxide nanoparticle treatment in a time-dependent manner.

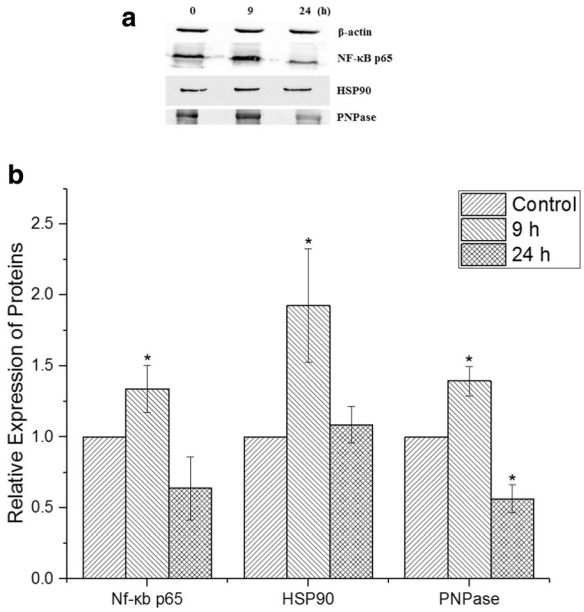

Fig. 4 Expression of NF-κB p65, HSP90, and PNPase at protein level

Intracellular reactive oxygen species

Intracellular ROS levels increased about 10% after A549 cells being treated with zinc oxide nanoparticles

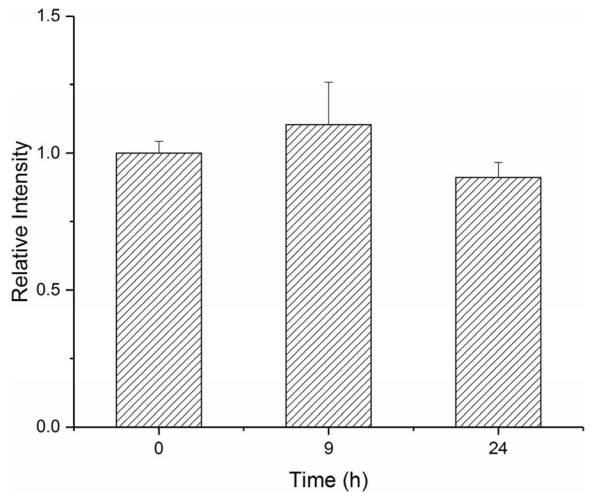

Fig. 5 Oxidative stress induced by exposure of A549 cells to 5 mg Zn/L ZnO nanoparticles after 0, 9, and 24 h

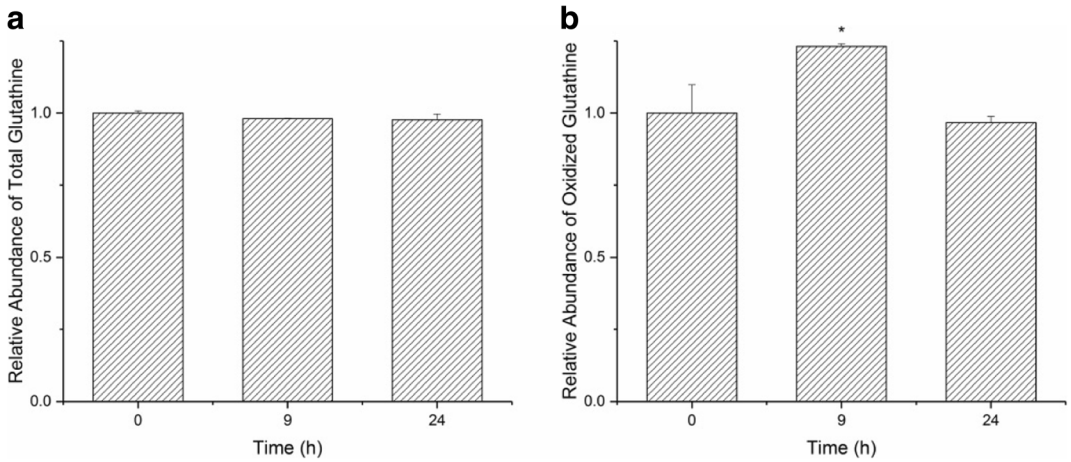

Fig. 6 **a** and **b** Time-dependent changes of total glutathione and oxidized glutathione in cells treated with ZnO nanoparticles

for 9 h, though no significant differences were discovered (Fig. 5). After 24 h of treatment, the intracellular ROS level fell back, slightly below the untreated level.

Intracellular glutathione/oxidized glutathione

Intracellular total glutathione/oxidized glutathione level was investigated in order to further verify the oxidative stress in A549 cells. As shown in Fig. 6, cellular total glutathione level maintained stable in the 24-h period, while oxidized glutathione increased significantly after cells being treated by zinc oxide nanoparticles for 9 h and then fell back at 24 h, which means the glutathione decreased after 9 h of treatment and then increased to control group level after 24 h.

Discussion

A549 cell viability shows responses to treatment with zinc oxide nanoparticles in a concentration-dependent manner, and the nanoparticles show cytotoxicity similar to zinc sulfate according to our previous work (Zhao, et al. 2015), in which zinc sulfate at the concentration of 150 μM (corresponding to 9.8 mg Zn/L) caused significant cell viability reduction after treatment for 24 h, while 10 mg Zn/L zinc oxide nanoparticles also induced significant cytotoxicity. Both 100 μM zinc sulfate (corresponding to 6.5 mg Zn/L) and 5 mg Zn/L zinc oxide nanoparticles caused minor cell viability reduction in A549 cells after 24 h. In addition, differences in cytotoxicity were also observed. Five hundred micromolars of zinc sulfate (corresponding to 32.7 mg Zn/L) treatment resulted in nearly 80% cell death, while 50 mg Zn/L zinc oxide nanoparticles only caused about 40% cell viability loss, which indicated that zinc ions induced higher cytotoxicity than zinc oxide nanoparticles at high concentration. Besides, zinc oxide nanoparticles dissolved incompletely after 24 h, and this ensured the basis of differences in toxicity mechanism. On the other hand, cytotoxicity induced by 25 mg Zn/L and 50 mg Zn/L zinc oxide nanoparticles was similar. In such high concentration, nanoparticle aggregation is unavoidable unless aggregation inhibitor is involved, which means that the specific surface area will decrease and cause less oxidative stress to cells and thus less cell viability loss. According to the result, 5 mg Zn/L zinc oxide nanoparticles were chosen for the following experiments since it is sub-cytotoxic and can further reveal cell homeostasis regulation in response to exogenous stimulation. Also, 9 h and 24 h were chosen so that we can make direct comparison between toxicity of zinc oxide nanoparticles and zinc sulfate.

One hundred twenty differentially expressed proteins were detected using iTRAQ assay and showed time-dependent expression patterns. Most (79) of 99 differentially expressed proteins after treatment with zinc oxide nanoparticles for 9 h were not detected to be differentially expressed after 24 h, which means that cells have managed to maintain homeostasis after treatment for 24 h. Among 20 proteins which showed to be differentially expressed both in 9 h and 24 h, 15 proteins were down-regulated in 9 h but the regulation was then suppressed, and the suppression was supposed to continue, which led to the expression level same to the untreated group after longer period of time. This result correlates

with our previous conclusion that protein expression changed largest after 9 h of treatment. Moreover, much more differentially expressed proteins were detected at 9 h than 24 h which also supports the conclusion and further reveals the importance of treatment time in mechanism of cellular response to zinc oxide nanoparticles. In addition, most of differentially expressed proteins were found to be down-regulated, and down-regulated proteins also outnumbered up-regulated proteins among 20 differentially expressed proteins after both 9 h and 24 h. By contrast, most of differentially expressed proteins in response to zinc sulfate were up-regulated (Zhao, et al. 2015), which showed a different toxicity mechanism. Also, differentially expressed proteins were involved in different biological processes to some extent, which is evidence that nanoparticle is crucial in the cytotoxicity even at low concentration.

ROS plays an important role in nanoparticle toxicity (Nel, et al. 2006). In order to evaluate the cytotoxicity originating from ROS, DCFH-DA fluorescent probes were used to determine the intracellular ROS level after A549 cells being treated with zinc oxide nanoparticles for 9 h and 24 h. It is shown that the ROS level increased about 10% after treatment for 9 h though no significant difference could be found, and then decreased to the level similar to control group. We further investigate the level of intracellular total glutathione and oxidized glutathione. Total glutathione level maintained stable in the 24-h treatment period while oxidized glutathione level increased significantly after treatment for 9 h and then fell back after 24 h. These results indicated that ROS were generated after cells being treated with zinc oxide nanoparticles and cell would respond to the oxidative stress, and the ROS level was suppressed to normal level after 24 h. These results corresponded to our proteomic results, and it is clear that cells sustained the homeostasis and the exogenous interference was suppressed after 24 h treatment, which is reasonable since the concentration chosen was sub-cytotoxic and a totally different outcome can be predicted if higher concentration was taken in the treatment.

Three proteins involved in related cell signaling pathways, NF-κB p65, PNPase, and HSP90 expression, were determined using western blot and they showed similar expression pattern, which corresponded to the conclusion that most proteins showed the greatest changes after 9 h of treatment. NF-κB is a multifunction transcription factor and presents in almost all types of cells. It participates in various biological processes including inflammation, immunity, apoptosis, proliferation, differentiation, and tumorigenesis and plays an important role in innate and acquired immune responses. NF-κB is a protein family, in which p65 is one of highest abundant proteins. Normally, p65 presents as a protein complex in cytoplasm and combined with NF-kappa-B inhibitor (IκB) family. After receiving an immune signal like TNF, IL-1, LPS, or other stimuli like virus and ultraviolet radiation, IκB kinase will promote the phosphorylation of IκB and cause it to degrade, and thus activate the NF-κB, which will transfer into cell nuclei and initiate the transcription process (Baldwin, 1996; Okamoto, et al. 1997; Karin and Ben-Neriah, 2000; Ghosh and Karin, 2002). Nanoparticles have been proved to induce the generation of ROS directly and ROS can activate various immunoreactions and lead to the activation of NF-κB p65 (Nel, et al. 2006; Yang, et al. 2013; Fooksman, et al. 2010). The main function of PNPase is to catalyze the phosphorolysis of purine nucleosides and deoxynucleosides to their respective purine bases and pentose-1-phosphates. Lack of PNPase will cause deficiency in purine catabolism and lead to immunological diseases. On the other hand, PNPase was also proved to be induced by ROS (Ealick, et al. 1990; Rao, et al. 1990). The significant increase of NF-κB p65 and PNPase indicates that the nanoparticle accounts for an important part in the toxicity of zinc oxide nanoparticles. HSP90 protein family shows a high-level expression in all types of cells. It is a chaperone protein that assists other proteins to fold properly and aids in degradation of misfolded proteins, so it is synthesized to deal with denatured proteins when cells encounter exogenous stimuli like high temperature, anoxia, and heavy metal (Csermely, et al. 1998). HSP90 increased significantly after cells being treated with 5 mg Zn/L zinc oxide nanoparticles for 9 h, and then declined to control group level after 24 h. However, when facing zinc sulfate stimuli in our previous work, HSP90α increased significantly after treatment for both 9 h and 24 h, and the expression at 24 h was even higher than 9 h. Considering HSP90 family responds to most of stimuli, combined with other results in our present work, we deducted that zinc oxide nanoparticles tend to have an "acute" effect on A549 cells while zinc ions will have a long-lasting effect on cells. This may be because more time is needed to regulate the concentration of intracellular zinc ions, while oxidative stress induced by ROS, which is originated from particles, can be abolished in a short period of time through regulation. This deduction

reveals the importance of controlling the time of treatment in the study of metal oxide nanoparticle toxicity mechanism. A long-time treatment may lead to the conclusion that metal ion-induced toxicity is the main contributor to metal oxide nanoparticle toxicity since particle-induced toxicity, which largely comes from ROS, can be abolished rapidly. The dissolving nanoparticles will cause the reduction of nanoparticle toxicity and the increase of metal ion toxicity, and vice versa. However, if cells fail to eliminate the excess ROS due to various reasons, for instance, being treated with metal oxide nanoparticles at high concentration, accumulated ROS may emphasize the toxicity induced by particle. The deduction can explain zinc oxide nanoparticle toxicity mechanism in this work properly.

Conclusions

Proteomes of A549 cells in response to zinc oxide nanoparticles stimulation after different period of time were profiled and the differentially expressed proteins are mainly involved in biological processes like transcription translation and protein folding. Although similar cytotoxicity was observed at low concentration, differences between cells in response to zinc oxide nanoparticles and zinc sulfate were investigated through cell viability assay and protein expression analysis. In addition, more differentially expressed proteins, more significant changes, and higher ROS level after treatment for 9 h than 24 h reveal the process of cell regulation in homeostasis maintenance. We further make a deduction that toxicity of nanoparticles consists both of particle toxicity and ion toxicity. When at low concentration, cells will suffer from particle and metal ion toxicity simultaneously for a short period of time, and then particle-induced toxicity will soon be relieved or eliminated through regulation, while dissolved metal ions may cost a long time to regulate. As a result, long-time treatment may conceal the toxicity induced by particles and in turn highlight the toxicity of metal ions. Still, some other causes which generate or suppress the elimination of ROS will lead to the ion toxicity and should be taken into consideration. This hypothesis tries to explain the controversies in explanations of zinc oxide nanoparticle toxicity mechanism and to reveal the significance of the exposure time in the study of metal oxide nanoparticle toxicity, which may provide a new perspective for studying toxicity mechanism of nanoparticles.

Funding This work was supported by the National Natural Science Foundation of China (91643105, 21577057, 91543129, 81072712, and 90913012), the Natural Science Foundation of Jiangsu Province (BK20171335), and the National Basic Research Program of China (973 program, 2011CB911003). We thank Mr. LY Huang for assistance in the ICP-MS determination of zinc.

Compliance with ethical standards

Conflict of interest The authors declare that they have no conflict of interest.

References

Baldwin AS (1996) The NF-kappa B and I kappa B proteins: new discoveries and insights. Annu Rev Immunol 14:649–683. https://doi.org/10.1146/annurev.immunol.14.1.649

Chang C, Chen S, Ho S, Yang CY, Wang HD, Tsai ML (2007) Proteomic analysis of proteins from bronchoalveolar lavage fluid reveals the action mechanism of ultrafine carbon black-induced lung injury in mice. Proteomics 7:4388–4397. https://doi.org/10.1002/pmic.200700164

Cho WS, Duffin R, Thielbeer F, Bradley M, Megson IL, MacNee W, Poland CA, Tran CL, Donaldson K (2012) Zeta potential and solubility to toxic ions as mechanisms of lung inflammation caused by metal/metal oxide nanoparticles. Toxicol Sci 126:469–477. https://doi.org/10.1093/toxsci/kfs006

Csermely P, Schnaider T, Soti C, Prohászka Z, Nardai G (1998) The 90-kDa molecular chaperone family: structure, function, and clinical applications. A comprehensive review. Pharmacol Ther 79:129–168. https://doi.org/10.1016/S0163-7258(98)00013-8

Deng X, Luan Q, Chen W, Wang Y, Wu M, Zhang H, Jiao Z (2009) Nanosized zinc oxide particles induce neural stem cell apoptosis. Nanotechnology 20:115101. https://doi.org/10.1088/0957-4484/20/11/115101

Ealick SE, Rule SA, Carter DC, Greenhough TJ, Babu YS, Cook WJ, Habash J, Helliwell JR, Stoeckler JD, Parks RE Jr, Chen SF, Bugg CE (1990) Three-dimensional structure of human erythrocytic purine nucleoside phosphorylase at 3.2 Å resolution. J Biol Chem 265:1812–1820. https://doi.org/10.1111/j.1749-6632.1985.tb27124.x

Fooksman DR, Vardhana S, Vasiliver-Shamis G, Liese J, Blair DA, Waite J, Sacristán C, Victora GD, Zanin-Zhorov A, Dustin ML (2010) Functional anatomy of T cell activation and synapse formation. Annu Rev Immunol 28:79–105. https://doi.org/10.1146/annurev-immunol-030409-101308

Ghosh S, Karin M (2002) Missing pieces in the NF-kappa B puzzle. Cell 109:S81–S96. https://doi.org/10.1016/S0092-8674(02)00703-1

Hackenberg S, Scherzed A, Technau A, Kessler M, Froelich K, Ginzkey C, Koehler C, Burghartz M, Hagen R, Kleinsasser N (2011) Cytotoxic, genotoxic and pro-inflammatory effects of zinc oxide nanoparticles in human nasal mucosa cells in vitro. Toxicol Vitro 25:657–663. https://doi.org/10.1016/j.tiv.2011.01.003

Huang CC, Aronstam RS, Chen DR, Huang YW (2010) Oxidative stress, calcium homeostasis, and altered gene expression in human lung epithelial cells exposed to ZnO nanoparticles. Toxicol. Vitro 24:45–55. https://doi.org/10.1016/j.tiv.2009.09.007

Jeng HA, Swanson J (2006) Toxicity of metal oxide nanoparticles in mammalian cells. J Environ Sci Health, Part A: Tox Hazard Subst Environ Eng 41:2699–2711. https://doi.org/10.1080/10934520600966177

Karin M, Ben-Neriah Y (2000) Phosphorylation meets ubiquitination: the control of NF-kappa B activity. Annu Rev Immunol 18:621–663. https://doi.org/10.1146/annurev.immunol.18.1.621

Laemmli UK (1970) Cleavage of structural proteins during the assembly of the head of bacteriophage-T4. Nature 227:680–685. https://doi.org/10.1038/227680a0

Lin WS, Huang YW, Zhou XD, Ma Y (2006) In vitro toxicity of silica nanoparticles in human lung cancer cells. Toxicol App Pharm 217:252–259. https://doi.org/10.1016/j.taap.2006.10.004

Lin W, Xu Y, Huang CC, Ma YF, Shannon KB, Chen DR, Huang YW (2009) Toxicity of nano- and micro-sized ZnO particles in human lung epithelial cells. J Nanopart Res 11:25–39. https://doi.org/10.1007/s11051-013-1829-5

Meyer DE, Curran MA, Gonzalez MA (2009) An examination of existing data for the industrial manufacture and use of nanocomponents and their role in the life cycle impact of nanoproducts. Environ Sci Technol 43:1256–1263. https://doi.org/10.1021/es8023258

Nel A, Xia T, Madler L, Li N (2006) Toxic potential of materials at the nanolevel. Science 311:622–627. https://doi.org/10.1126/science.1114397

Okamoto T, Sakurada S, Yang JP, Merin JP (1997) Regulation of NF-kappa B and disease control: identification of a novel serine kinase and thioredoxin as effectors for signal transduction pathway for NF-kappa B activation. Curr Top Cell Regul 35:149–161. https://doi.org/10.1016/S0070-2137(97)80006-4

Park E, Yi J, Chung Y, Choi J, Park K (2008) Oxidative stress and apoptosis induced by titanium dioxide nanoparticles in cultured BEAS-2B cells. Toxicol Lett 180:222–229. https://doi.org/10.1016/j.toxlet.2008.06.869

Prach M, Stone V, Proudfoot L (2013) Zinc oxide nanoparticles and monocytes: impact of size, charge and solubility on activation status. Appl Pharmacol 266:19–26. https://doi.org/10.1016/j.taap.2012.10.020

Rao PN, Walsh TR, Makowka L, Rubin RS, Weber T, Snyder JT, Starzl TE (1990) Purine nucleoside phosphorylase: a new marker for free oxygen radical injury to the endothelial cell. Hepatology 11:193–198. https://doi.org/10.1002/hep.1840110206

Sharma V, Anderson D, Dhawan A (2011) Zinc oxide nanoparticles induce oxidative stress and genotoxicity in human liver cells (HepG2). J Biomed Nanotechnol 7:98–99. https://doi.org/10.1166/jbn.2011.1220

Song WH, Zhang JY, Guo J, Zhang J, Ding F, Li L, Sun Z (2010) Role of the dissolved zinc ion and reactive oxygen species in cytotoxicity of ZnO nanoparticles. Toxicol Lett 199:389–397. https://doi.org/10.1016/j.toxlet.2010.10.003

The Project on Emerging Nanotechnologies Consumer Products Inventory. Available at http://www.nanotechproject.org/inventories/consumer/

Triboulet S, Aude-Garcia C, Armand L, Gerdil A, Diemer H, Proamer F, Collin-Faure V, Habert A, Strub JM, Hanau D, Herlin N, Carri re M, Van Dorsselaer A, Rabilloud T (2014) Analysis of cellular responses of macrophages to zinc ions and zinc oxide nanoparticles: a combined targeted and proteomic approach. Nanoscale 6:6102–6114. https://doi.org/10.1039/C4NR00319E

Xia T, Kovochich M, Liong M, Mädler L, Gilbert B, Shi H, Yeh JI, Zink JI, Nel AE (2008) Comparison of the mechanism of toxicity of zinc oxide and cerium oxide nanoparticles based on dissolution and oxidative stress properties. ACS Nano 2:2121–2134. https://doi.org/10.1021/nn800511k

Yang YH, Bazhin AV, Werner J, Karakhanova S (2013) Reactive oxygen species in the immune system. Inter Rev Immunol 32:249–270. https://doi.org/10.3109/08830185.2012.755176

Zhao WJ, Song Q, Wang YH, Li KJ, Mao L, Hu X, Lian HZ, Zheng WJ, Hua ZC (2014) Zn-responsive proteome profiling and time-dependent expression of proteins regulated by MTF-1 in A549 cells. PLoS One 9:e105797. https://doi.org/10.1371/journal.pone.0105797

Zhao WJ, Song Q, Zhang ZJ, Mao L, Zheng WJ, Hu X, Lian HZ (2015) The kinetic response of the proteome in A549 cells exposed to ZnSO4 stress. PLoS One 10:e0133451. https://doi.org/10.1371/journal.pone.0133451

Zhong L, Yu Y, Lian HZ, Hu X, Fu H, Chen YJ (2017) Solubility of nano-sized metal oxides evaluated by using in vitro simulated lung and gastrointestinal fluids: implication for health risks. J. Nanopart. Res 19:375. https://doi.org/10.1007/s11051-017-4064-7